# Flow Bifurcation Phenomena of Shear-Thinning and Newtonian Fluids in a Rectangular Channel in Presence of Intermediate Steps: using Carreau-Yasuda Model

S. Saha[1†] and A. N. Das[2]

*[1] Department of Mathematics, NIT Silchar, Silchar, Assam, 788010, India*
*[2] Department of Mathematics, Alipurduar College, Alipurduar, West Bengal, 736121, India*

†*Corresponding Author Email: sandip.tfgss@gmail.com*

## ABSTRACT

Flow bifurcation transitions of shear-thinning fluid and Newtonian fluid, flow through a two-dimensional rectangular channel in presence of intermediate steps have been considered in this manuscript. Employing SIMPLE algorithm, the governing equations have been solved numerically and using FLUENT software to visualize the simulation results for convenience. The Rheological properties of shear-thinning and Newtonian fluids are described in the light of Carreau-Yasuda model. The result of this formulation has been validated with those of an earlier work. The motivation of this work is to study the bifurcation characteristics for different values of Reynolds numbers in presence of multiple steps in a rectangular channel. Pressure drop characteristic has also been studied for different values of expansion ratio and intermediate steps. For some particular value of expansion ratio (ER), a linear relation between $Re_{crit}$ and the value of $n$ of Carreau-Yasuda model has been shown.

Keywords: Rectangular channel; Shear-thinning fluid; Newtonian fluid; Flow bifurcation; Carreau-Yasuda model.

## NOMENCLATURE

| | | | |
|---|---|---|---|
| $L_u$ | inlet length | $\rho$ | density |
| $L_d$ | outlet length | $\eta$ | dynamic viscosity |
| $Re_{crit}$ | critical values of Reynolds number | $h_u$ | upstream channel length |
| ER | expansion ratio= $L_d/L_u$ | $Re$ | Reynolds number $= \frac{\rho v_{mean} L_u}{\eta_0}$ |
| n | index number in Carreau-Yasuda model | | |
| s | intermediate step | $\eta_0$ | low shear rate of viscosity |
| $h_d$ | downstream channel length | $\Delta p$ | absolute pressure drop $=|(p_2-p_1)|$ |
| $v_{mean}$ | average inlet velocity | A | strain velocity tensor |
| p | pressure | $\dot{\gamma}$ | shear rate |
| c, n | model parameters | $\eta(\dot{\gamma})$ | dynamic viscosity at shear rate |
| $p_1$ | pressure at inlet section | $\eta_\infty$ | high shear rate of viscosity |
| $p_2$ | pressure at outlet section | $\eta_{Lu}$ | average viscosity of Carreau-Yasuda fluid |
| $H_i$ | normalized corner vortex length | $p_{rf}$ | pressure recovery factor $= \sqrt{p_2 - p_1}$ |
| $h_i$ | corner vortex length | | |
| $Re_N$ | Reynolds number for Newtonian model | | |
| $v_{in}$ | velocity inlet | | |

## 1. INTRODUCTION

Flow through a rectangular channel in presence of intermediate steps in the inlet section behaves similar to sudden expansion channel which has many practical applications in the field of science and technology. Biomedical (Liepsch 2002), and chemical flows through sudden expansion channel are highly encountered in industrial equipment (Joseph and Allen 1996) such as air conditioning system, heat exchangers (Konoplev *et al.* 2007, Motaharinezhad *et al.* 2014) hydraulic controls, etc. It has also a numerous pragmatic real-life applications on medical science such as pulmonary,

cardiovascular flow systems as well as in arterial stenoses (Casas *et al*. 2016, Mao *et al*. 2011, Peterson *et al*. 2008, Peterson *et al*. 2016, Vtel *et al*. 2008). Moreover, it is more prevalent in the mixing of incompatible polymers (Mukhambetiyar *et al*. 2017) and also applicable to investigate the effect of high-velocity jets (Litvinenko *et al*. 2014, Mostafavi *et al*. 2017). It is also of particular interest to use a sudden expansion channel for turbulence flows for lower values of Reynolds number (Das *et al*. 2015, Durst *et al*. 1974, Fattah 2012, Neofytou and Drikakis 2003, Oliveira 2008, Tsai *et al*. 2007, Vinogradov *et al*. 2011). In a sudden expansion channel, many authors (Ameur *et al*. 2018, Cherdron *et al*. 1978, Fearn *et al*. 1990, Mandal *et al*. 2011, Menouer *et al*. 2019, Mishra *et al*. 2002, Oliveira 2003, Poole *et al*. 2007, Quadros *et al*. 2018, 2020, Ringleb *et al*. 2018, Saha *et al*. 2020, Torres *et al*. 2020) have investigated the structure of flows using various types of fluids. They showed that vortices are formed near the expansion zone of the channel and those become larger and expanded with the increase in the values of *Re*. It is also described in their work that after attaining a certain value of *Re*, flow breaks the symmetry which in turn form different lengths of vortices till it reached to a developed turbulent flow, which is known as flow bifurcation.

Ternik (2010) numerically studied the laminar flow regime for a wide range of *Re* in a 1:3 two-dimensional sudden expansion channel. Using power-law index (0.60 ≤ n ≤ 1.40), he studied the recirculation length, and Couette correction for both the shear-thinning and shear-thickening fluids and concluded that attached and detached points are influenced by non-Newtonian viscous behavior of the fluid. Also for shear-thinning fluids, he revealed that an increase of Power-law index causes the increase of recirculation length and in case shear thickening fluids, reattachment length varies linearly with the increase of *Re*. Ternik (2009) numerically studied the flow transition from symmetry to asymmetry for *Re* ranges between 10 to 150 considering purely viscous shear-thinning fluids. In terms of pressure gradients, pressure drop, vortex lengths, values of $Re_{crit}$ and the resistance of flow he found that shear thinning fluid influenced highly than the Newtonian fluid.

Study of $Re_{crit}$ in a 1:3 sudden expansion channel was done by Ternik *et al*. (2006) numerically, using the Quadratic model (Marn and Ternik 2003). To study the shear-thickening behavior of corn-starch and water mixture they employed both the Quadratic and Power-law models and found a good relationship of the results of the models. Furthermore, they stated that flow asymmetry is highly influenced by shear-thickening fluid behavior. Bell *et al*. (1994) studied the Shear-Thinning and Shear-Thickening fluid flows for Power-law indices n( ≠1) in a 1:2 symmetric sudden expansion channel. In their work, it is also shown that flow asymmetry arises when n > 1. Hammad *et al*. (2001) numerically investigated the non-Newtonian Herschel-Bulkley fluids for the Power law index 0.6 ≤ n ≤ 1.2. The finite difference

method was employed to investigate the shear-thinning, shear thickening effects on flow patterns and found an inverse relationship between the Power law index (n) and recirculation region length.

Up to now, most of the researchers have solved many problems considering the variation of expansion ratio. It is to mention that the effect of the presence of intermediate step in the inlet of the rectangular channel has not been considered so far. Therefore it will be of great interest to study the characteristics of the velocity profile and pressure drop in the rectangular channel in presence of intermediate steps. Another interesting thing is to study the impact of intermediate steps in the inlet section of a channel on $Re_{crit}$. The present study investigates that the flow phenomena of Newtonian and shear-thinning fluids through a two-dimensional rectangular channel in presence of intermediate steps in the inlet of the channel. To analyze the flow bifurcation phenomena, 0.2 wt% aqueous solution of xanthan gum (Haase *et al*. 2017) has been considered. The Carreau-Yasuda model has been considered to study the flow rheological behavior. At $Re=200$, n = 1 and ER=3, normalized velocity profile and pressure profile have been investigated for s= 1, 2 and 4. Numerical calculations are carried out for a wide range of $Re \in [0.1-250]$ with different values of n from 0 to 1. Moreover, the present study investigates the flow bifurcation transition (symmetric to asymmetric) at each s = 1, 2 and 4. Furthermore, the critical values of Reynolds number have been studied for various shear-thinning fluids (n < 1) and Newtonian fluid (n = 1). Formulation of the problem of this paper is as follows: section 2 describes the Carreau-Yasuda model, whereas the model geometry, governing equations, numerical procedure and grid test are given in sections 3, 4, 5 and 6, and numerical results are depicted in the form of graphs in section 7, lastly the conclusion is drawn in section 8.

## 2. CARREAU-YASUDA MODEL

In literature review, it has been found that most of the researchers (Bell *et al*. 1994, Hammad *et al*. 2001, Ternik *et al*. 2006, Ternik 2009, 2010) used Power-law model to describe the rheological properties of shear-thinning fluids, which is formulized as follows:

$$\eta(\dot{\gamma}) = c\dot{\gamma}^{n-1} \qquad (1)$$

But it has some disadvantages; it assumes an infinite increase in viscosity with a reduction in shear rate but does not explain the transition towards a Newtonian fluid with a constant viscosity in most shear-thinning fluids. Moreover, Eq. (1) presents that at high shear rates viscosity tends to zero. To overcome these disadvantages, the Carreau-Yasuda model has been employed in this current work which is formulated as below:

$$\eta(\dot\gamma) = \eta_\infty + (\eta_0 - \eta_\infty)\left[1 + (\lambda\dot\gamma)^a\right]^{\frac{(n-1)}{a}} \quad (2)$$

The parameter values $\eta_0$, $\eta_\infty$, $\lambda$ and $a$ are taken in accordance to Haase *et al*. (2017). At sufficiently low viscosity and high shear rate ($(\lambda\dot\gamma)^a \gg 1$) and $\eta_\infty$ tending to zero), Carreau-Yasuda formulation can be transformed into Power-law formulation written earlier with, $c = \eta_0 \lambda^{n-1}$. Various authors (Haase *et al*. 2017, Boyd *et al*. 2007) have solved many problems using this model.

### 3. Model geometry

The abrupt changes in the flow passage in the middle section of the inlet of the rectangular channel causes the existence of turbulent eddies which leads to higher energy loss. In the present analysis, intermediate steps (s= 1, 2, and 4) have been implemented to get the same expansion flow, but to obtain a different feature of flow depletion. The flow field of Shear-Thinning fluid (*n*<1) and Newtonian fluid (n = 1) have been considered in a two-dimensional rectangular channel in the presence of intermediate steps, which are depicted in Figs. 1(a-c). Flow geometries [Figs. 1(a-c)] are described in a Cartesian coordinate system (x, y) for ER= 3. Center of the coordinate system lies in the center of the model geometry as shown in Figs. 1(a-c) where $h_d = 50L_u$ and $h_u = 2L_u$.

### 4. Governing equations

The incompressible shear thinning fluid flows through a two-dimensional rectangular channel in presence of intermediate steps are governed by following continuity and generalized Cauchy equations.

$$\nabla.v = 0 \quad (3)$$

$$\rho\left[\frac{\partial v}{\partial t} + (v.\nabla)v\right] = -\nabla p + \nabla[\eta(I_2)A] \quad (4)$$

Here, $\eta(I_2)$ be the viscosity of non-Newtonian fluid which is a function of second invariant of strain velocity tensor, where [$I_2$ = A: A]. In this work $\rho$ is set to 1000 kg/m$^3$ (Assis *et al*. 2010, Haase *et al*. 2017) and A= $\dfrac{(\nabla v + (\nabla v)^T)}{2}$. The Eq. (2) can be written in the following form.

$$\eta(I_2) = \eta_\infty + (\eta_0 - \eta_\infty)\left[1 + \left(2\lambda^2 I_2\right)^{\frac{a}{2}}\right]^{\frac{(n-1)}{a}} \quad (5)$$

Again Eq. (5) can be rewritten in terms of equation in terms of average viscosity of Carreau-Yasuda fluid:

$$\eta_{L_u} = \eta_\infty + (\eta_0 - \eta_\infty)\left[1 + \left(\lambda v_0 L_u^{-1}\right)^a\right]^{\frac{(n-1)}{a}} \quad (6)$$

At n= 1, the above Eq. (6) leads to $\eta_{L_u} = \eta_0$, which is the general definition of *Re* for Newtonian fluid flow with viscosity $\eta_0$.

### 4.1. Boundary conditions

In this section the velocity and pressure fields on the boundaries of three sections e. g., inlet, outlet sections and wall boundary are specified as follows:

1.  Inlet section: Velocity inlet, x/$L_u$=-2,

-0.5<y/$L_u$<0.5: v= $v_{in}$, where $v_{in}$ lies between [0.0089-0.1958] m/s for Re ranges between [10-220].

2.  Outlet section: $\dfrac{\partial v}{\partial x} = 0$ , at x/$L_u$= 50.

3.  Wall boundary conditions: At the walls of the channel $v_x$=0 (no slip condition) and $v_y$ = 0 (no penetration boundary condition).
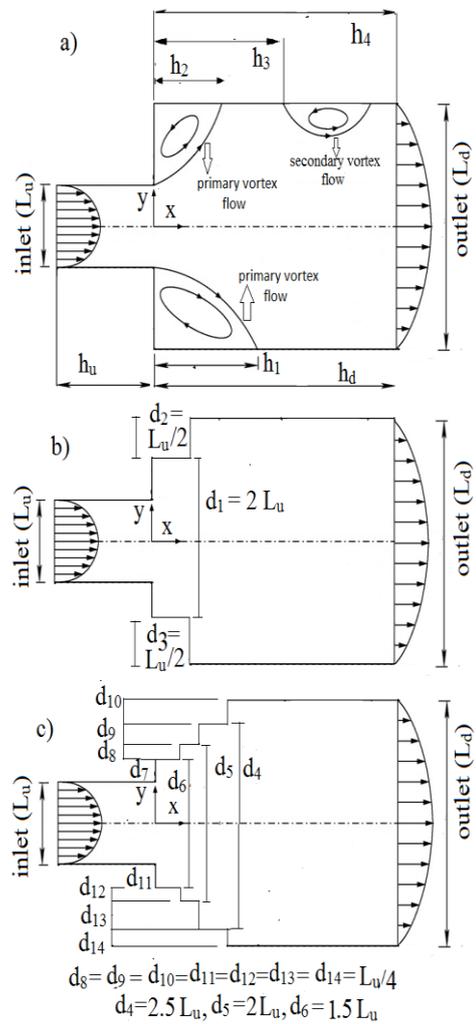


**Fig. 1. Rectangular flow geometry in presence of intermediate step, (a) s = 1, (b) s = 2, and (c) s = 4.**

## 4.2. Numerical procedure

Finite volume method (Safaei *et al.* 2011, Moghiman *et al.* 2008, Nourollahi *et al.* 2008, Rezaei *et al.* 2015) has been employed in this work to solve the governing equations. The integration over the set of controlling volumes forming the computational mesh discretized the governing equations in the space. Such a process entails, along with the constitutive equations, a linearized balance of mass and energy conservation. All the variables of the equations are evaluated and stored inside the control volume core (cells). Therefore to ensure pressure-velocity coupling, special numerical techniques are necessary. However there are some imperative characteristics of the finite volume method (e.g., solution that satisfies the conservation of quantities like mass, momentum, etc.), there have been various undesirable numerical effects (e.g., artificial diffusion) which are induced by lower order interpolation by convective terms. Second order upwind differencing scheme (QUICK) due to Leonard (1979), has been used to resolve these consequences as well as to discretize all the equations.
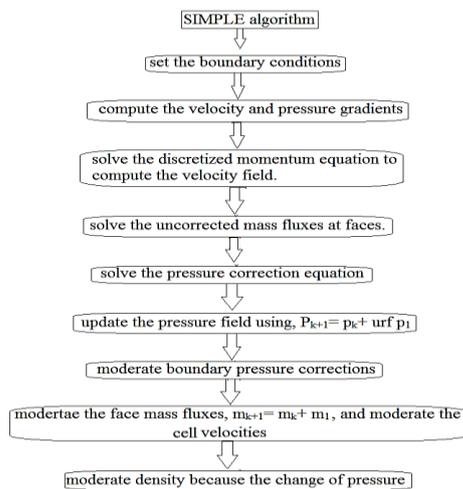


**Fig. 2. Flowchart of SIMPLE algorithm.**

This method has been employed to Newtonian, shear thinning and inelastic shear thickening fluids (Ternik *et al.* 2006; Ternik 2009) as well as to viscoelastic fluid flow (Edussuriya *et al.* 2004) with a view to efficiency and accuracy. In this presentation, SIMPLE algorithm (Patankar *et al.* 1980)) has been used for coupling pressure and velocity to achieve accurate results in the solution domain and the flowchart is shown in Fig. 2. FLUENT software is used to visualize the simulation results for convenience

## 5. Grid test and model validation

Grid test has been performed to select the number of mesh size of the whole computational domain [Figs. 1(a-c)]. Meshing of the whole computational domain [Figs. 1(a-c)] has been segregated into uniform rectangular meshes (Fig. 3). For this test, average pressure coefficients along the upper wall

has been analyzed for all the computational domain using pressure based solver taking $Re = 60$ and $ER = 3$. It is investigated that optimum number of cells are 60820 at s = 1, 60460 at s = 2 and 59423 at s = 4 for efficient and quantitative simulation, which are shown in Figs. 4(a-c).

Numerical results regarding the values of normalized velocity profiles and pressure profile at the centerline, obtained in this paper have been compared with those of Ternik *et al.* (2006). Figures 5(a-c) and at $Re_N = 50$, table 1 depicts a good agreement of the results of present work with those of Ternik *et al.* (2006).
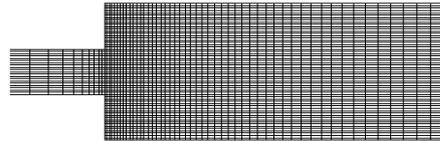


**Fig. 3. Mesh geometry.**

**Table 1 Percentage error of Ternik *et al.* (2006) vs present work at $Re_N = 50$.**

| | Ternik *et al.* (2006) | Present study | [(Ternik *et al.* 2006- Present study)/ Ternik *et al.* 2006] ×100 |
|---|---|---|---|
| Locatio n (x/h$_u$) | Dimensionless velocity | | Percentage error |
| 1.07 | 1.5974 | 1.596 | 0.087 |
| 1.69 | 1.2355 | 1.2352 | 0.024 |
| 2.34 | 0.9323 | 0.9320 | 0.032 |
| 3.71 | 0.4922 | 0.4921 | 0.020 |
| 6.66 | 0.2965 | 0.2964 | 0.033 |
| 9.52 | 0.2867 | 0.2864 | 0.100 |
| 12.3 | 0.2867 | 0.2866 | 0.034 |
| 16.48 | 0.2965 | 0.2964 | 0.033 |
| 19.02 | 0.2867 | 0.2865 | 0.069 |
| 24.31 | 0.2867 | 0.2866 | 0.035 |
| Total percentage error= 0.467% | | | |

## 6. Results and discussions

Using streamlines for various Re and different values of n, results of the numerical simulation of flow in the suddenly expanded micro-channel have been presented to show the impact of the existence of multiple intermediate steps in an abrupt geometry of expansion.

## 6.1. Flow structure for different various Re

In this section, discussions on separation and reattachment of corner vortices have been made for various values of *Re* in presence of intermediate steps in a rectangular channel at n = 1. For different values of s, the velocity streamlines for ER = 3 and $Re = 10, 55, 220$ have been presented in Figs. 6(a-c), 7(a-c) and 8(a-c) respectively and observed that the variation in velocity values with the number of steps are too small for $Re = 10$ but those decrease with the increase of the number steps for $Re = 55$,
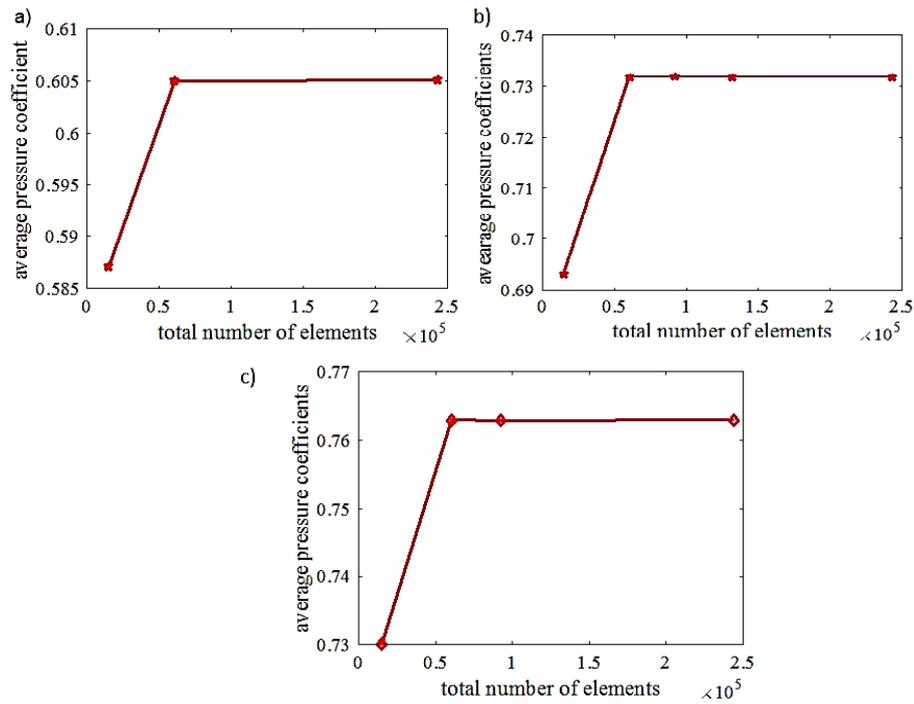
**Fig. 4. Average pressure coefficients along the upper wall for (a) s = 1, (b) s = 2 and (c) s = 4 at *Re* = 60.**
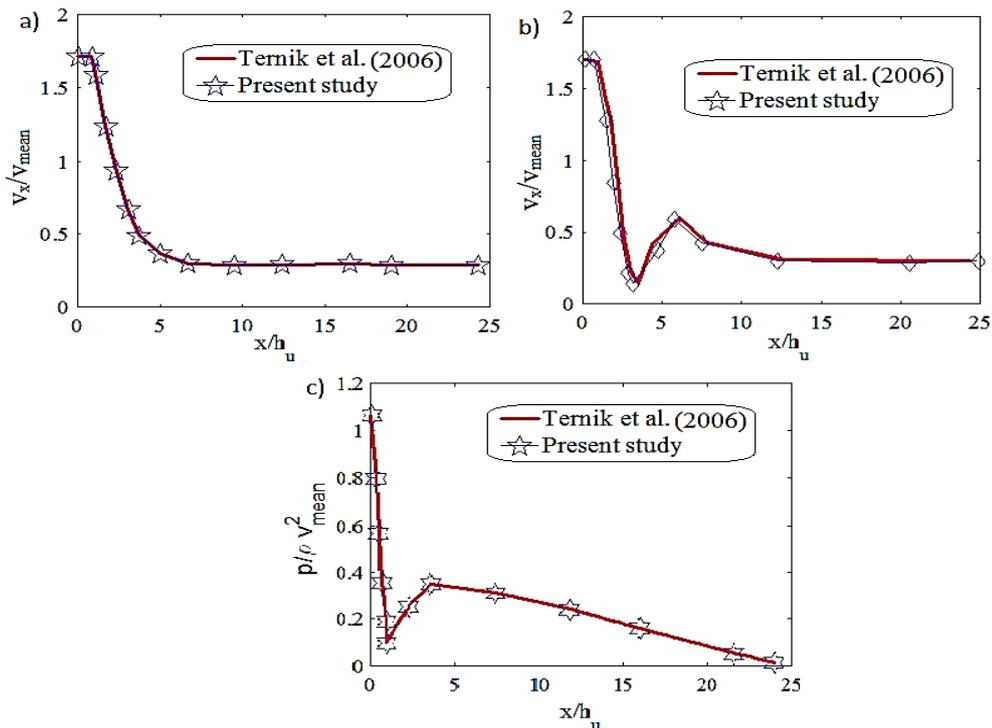


**Fig. 5. Normalized centerline velocity profiles at (a) *Re*N = 50, (b) *Re*N = 100 and normalized centerline pressure profile at (c) *Re*N = 50.**

220. For s = 1 [Fig. 6(a) and 7(a)], two corner vortices are formed at the corner walls of the channel. Near the upper wall of the channel, one vortex rotates in counter clockwise direction and another one rotates in clockwise direction near the lower wall of the sudden enlargement section which was also described by Ternik *et al.* (2009), Moallemi and Brinkerhoff (2006), and Pitton *et al.* (2017). Moreover, for s = 2, corner vortices are formed at each corner wall of the intermediate steps. It has been found that, at the upper and lower corner of the walls of the channel, four corner vortices are formed alternatively [Fig. 6(b) and 7(b)]. It is also observed that the length of the
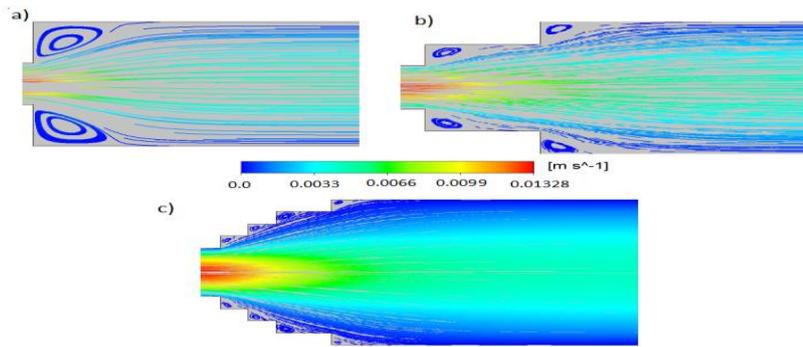
**Fig. 6. Velocity streamlines for (a) s = 1, (b) 2 and (c) 4 at $Re = 10$.**
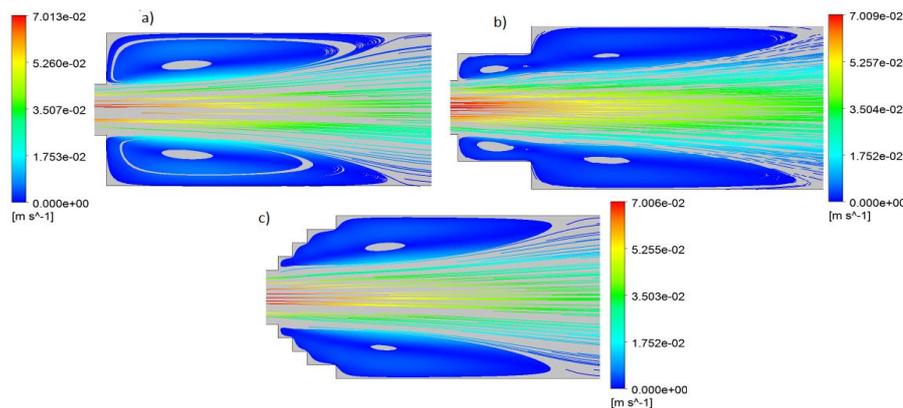


**Fig. 7. Velocity streamlines for (a) s = 1, (b) 2 and (c) 4 at $Re = 55$**

second corner vortex is larger than that of the first corner vortex. It has also been observed that the length of corner vortices increases with the increase of Reynolds number as well as with the increase of intermediate steps and also the flow creates the region of separation bubbles due to the increase of intermediate steps (s= 4). It has also been found that, number of corner vortices increases towards the downstream direction with the increase of Reynolds number as shown in Figs. 6(c), 7(c) and 8(c), but the overall length of vortices decreases with the increase of intermediate steps. In addition, for all the intermediate steps, it is found that when $Re < 60$, flow becomes symmetric at the horizontal axis of flow geometry and the flow becomes asymmetric when $Re > 60$ as shown in Fig. 8(a-c).

The recirculation zone is also found to increase in the downstream direction of the channel with the increase in the values of Reynolds number and for all the values of n, within the stable laminar region of the flow regime, flow vortices are strengthened with its expansion. Moreover, it is found that the flow becomes wavy [Fig. 6(c)-8 (c)] towards the downstream direction of the channel as the Reynolds number increases. For s= 1, 2, 4, it is clear from the streamlining plot for $Re = 220$ that the flows in all three cases are unstable as both the upper and the lower walls are of different sizes and symmetry of flow vortices disappears.

## 6.2. Effect of ER at n = 1

For different values of Reynolds number, Figs. 9(a-c) present bifurcation diagrams at $ER = 2, 3, 6$ respectively. In all the cases, it is observed that after a certain value of $Re$ ($Re < Re_{crit}$) flow breaks the symmetry. Consequently two corner vortices are formed with different lengths. For each fixed value of ER, it is also found that length of corner vortices linearly increases with the increase of $Re$. It has been observed that, at s = 1, flow breaks the symmetry when $Re < 130$ for ER = 2, and for ER = 3 the same occurs at $Re < 59.8$. But, for ER = 6, symmetry breaking bifurcation occurs when $Re < 44$. At s = 4, it is asserted that flow loses its stability when $Re < 158.3$, $Re < 70.6$, and $Re < 53.8$ for ER = 2, 3 and 6 respectively, which are clearly shown in Figs. 9(a-c) and 10. At each intermediate steps, it is revealed that as increase of ER causes the decrease of critical value of $Re_{crit}$ as shown in Fig. 11. From the further studies, it is noted that the distribution of corner separation zone causes the increase of recirculation region. Consequently, the length and height of recirculation region decreases.

## 6.3. Velocity and pressure profile at n = 1 and ER = 3

Along the centerline, the variation of normalized velocity and pressure profiles have been shown in Figs. 11(a-b) and found that normalized velocity
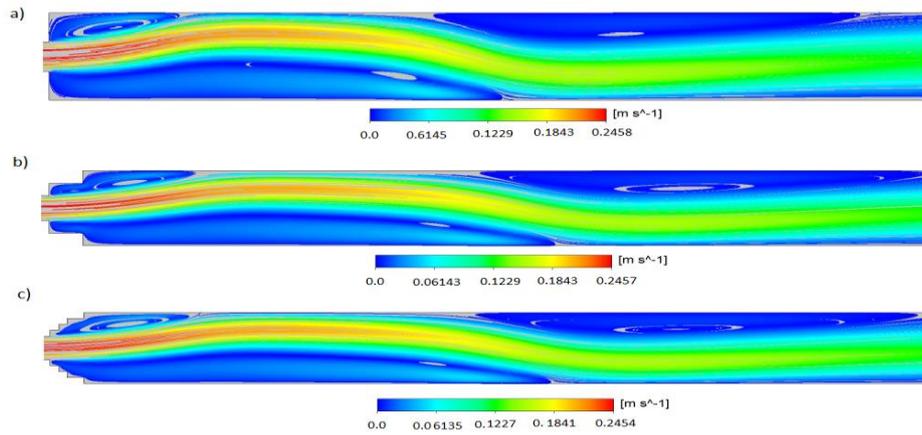
**Fig. 8. Velocity streamlines for (a) s = 1, (b) 2 and (c) 4 at $Re = 220$.**
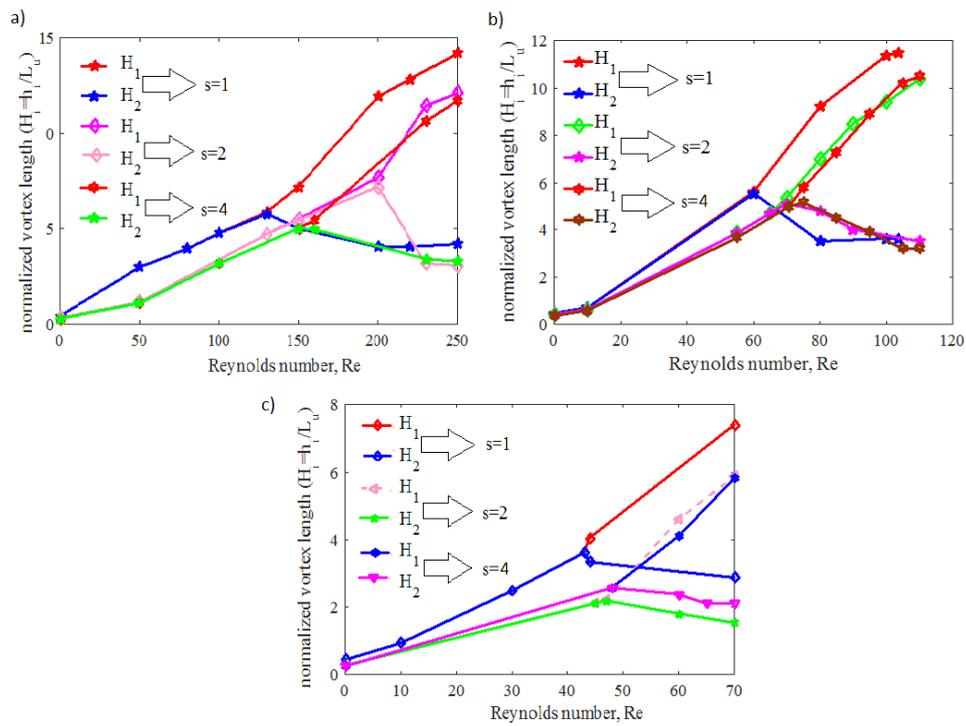


**Fig. 9. Bifurcation diagram for (a) ER = 2, (b) 3 and (c) 6 at n=1 for various $Re$.**
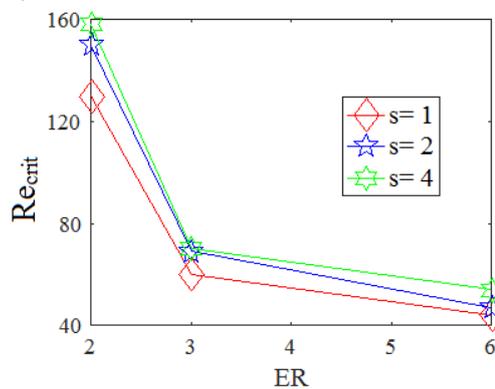


**Fig. 10. Profile of $Re_{crit}$ vs ER.**

component becomes zero at two positions at the downstream section of the channel. At $Re = 200$, similarity of centerline velocities are found for all values of s. Moreover, the span wise velocity fluctuation becomes almost zero after x = 16.7d at s=1. Along the centerline, it has also been found that, the velocity fluctuations decrease as the number of steps increases, which indicates the increased relative flow stability. Figure 11(b) shows the pressure distribution, for three different steps at $Re=200$ along the centerline of the expansion section. At ER = 3 and n = 1, the variation of absolute values of pressure drop has been presented for different values of s in Fig. 12(a). It is found that, as increase of number of steps causes the increase of absolute values of pressure drop as shown in Figs. 11(b) and 12(a). Moreover, it is
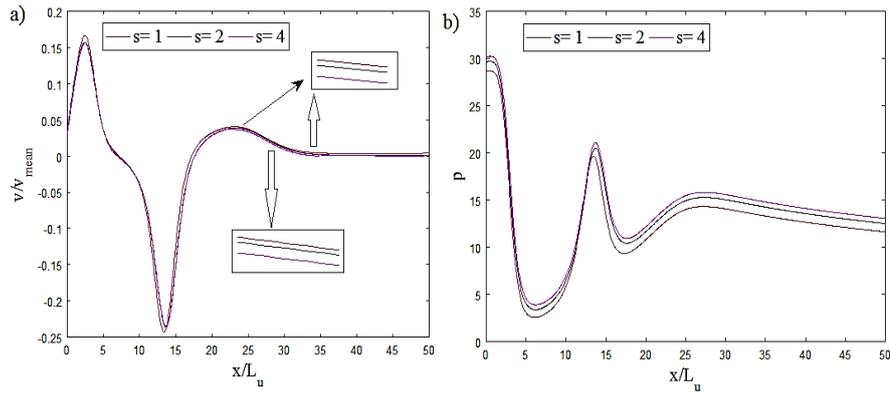
**Fig. 11. Normalized centerline (a) velocity profile and (b) pressure profile at n=1, $Re = 200$ and ER=3.**
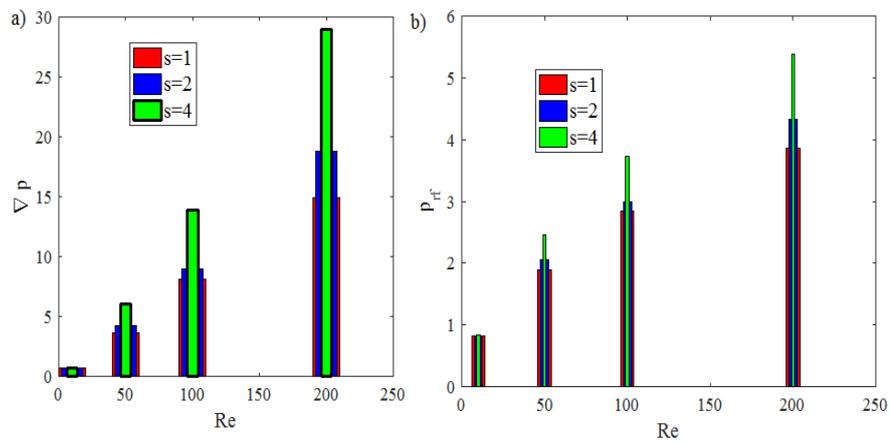


**Fig. 12. Absolute (a) pressure drop and (b) pressure recovery factor at n=1 and ER=3 for various $Re$.**
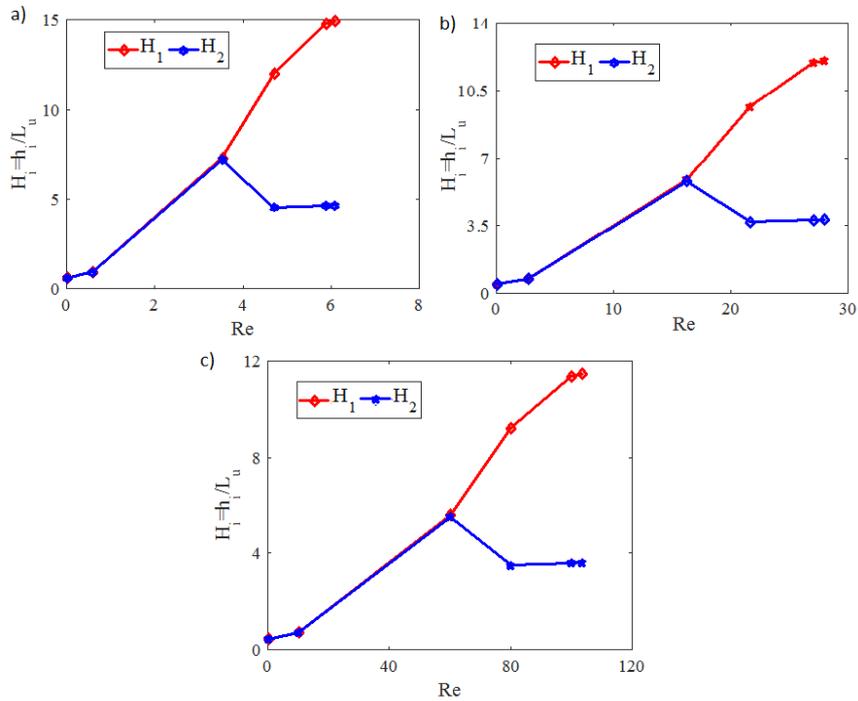


**Fig. 13. Bifurcation diagram for various shear-thinning [(a) n= 0], and (b) n= 0.8] and Newtonian fluids (n= 1) (c) at ER= 3 for different $Re$.**
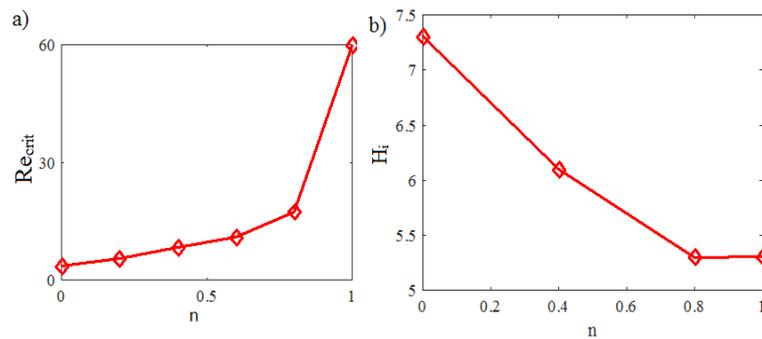
Fig. 14. Variation of (a) $Re_{crit}$ and (b) H$_i$ with different n at s=1.

observed that relative smoothness of pressure profiles increases with the increase in number of steps. The trend of the pressure recovery factor (p$_{rf}$) shown in Fig. 12(b) reflects a sudden expansion of the downstream flow. The increase of fluid static pressure can be noted as the fluid flows from the narrow section towards the outlet section. It is also noted that pressure recovery factor increases with the increase of number of steps. Higher pressure recovery and smoother pressure variations due to the presence of intermediate steps are presented in Fig. 12(b). In addition, for all the values of intermediate steps, it is observed that pressure recovery factor increases as the value of *Re* increases. At s= 4, it is found that pressure recovery factor becomes 1.4 times as compared to s= 1.

### 6.4. Effect of n at s = 1

The effect of Newtonian and Shear-thinning fluids has been discussed in this subsection at different values of n, which ranges between 0 to1. For both the Shear-thinning (n = 0 and 0.8) and Newtonian fluids (n = 1), it is observed that at smaller values of *Re*, flow becomes symmetric, which are shown in Fig. 13(a-c). Length of the recirculation region increases with the increase of *Re* until a certain value of *Re*, where the flow breaks the symmetry. It is revealed that, for n = 0, symmetry breaking bifurcation exists at *Re* = 3.5, but for n = 0.8, flow breaks the symmetry at *Re* = 16.53. It is also noted that $Re_{crit}$ becomes 59.8 in case Newtonian fluid (n = 1). Figure 14(a) presents an inverse relationship between $Re_{crit}$ and n. In addition, it has been studied that in case of shear-thinning fluids (n < 1), bifurcation transitions occur at low values of Reynolds number rather than Newtonian fluid (n = 1). From Fig. 14(b), it is clearly observed that the normalized vortex length (H$_i$) decreases with the increase of n.

### 7. Conclusion

In this work, mathematical modeling of the laminar flow of shear-thinning and Newtonian fluid flow through a rectangular micro-channel in presence of intermediate steps have been analyzed for different values of *Re* and ER, which has many applications in the field of science and technology and also in many industrial applications, like cooling equipments, fiber spinning, extrusion and medical instruments. Keeping the importance of the above applications in mind, an attempt has been made to solve the problem considered in this paper numerically. Effects of intermediate steps in different flow characteristics such as absolute value of pressure drop, pressure recovery factor and also on length of vortices, flow symmetry, centerline velocity for a flow through an expansion channel have been described in detailed in this paper. The effects of the parameter n, used in this model, on normalized vortex length, critical values of Reynolds number, expansion ratio have also been presented in the form of graphs showing that how the presence of steps affected different parameters. It is to be mentioned that for shear-thinning fluids, bifurcation transition occur for small values of Reynolds number as compared to the case of Newtonian fluid and at some Reynolds number, a bifurcation flow occurs and the symmetry of the flow between the upper and lower halves is lost.

### CONFLICT OF INTEREST

No conflict of interest

### REFERENCES

Ameur, H. (2018). Pressure Drop and Vortex Size of Power Law Fluids Flow in Branching Channels with Sudden Expansion. *Journal of Applied Fluid Mechanics* 11(6), 1739-1749.

Assis, F. T., E. E. G. Rojas, G. C. Guimares, M. C. Coelho, A. V. Ramos, B. S. Costa and R. S. J. Coimbra (2010). Kinematic Viscosity and Density of Binary and Ternary Mixtures Containing Hydrocolloids, Sodium Chloride, and Water. *International Journal of Thermophysics* 31, 513-524.

Bell, C. B. and K. S. Surana (1994). pVersion least squares finite element formulation for two-dimensional, incompressible, non-Newtonian isothermal and non- isothermal fluid flow. *International Journal for Numerical Methods in Fluids* 18, 127-162.

Boyd, J., J. M. Buick and S. Green (2007). Analysis of the Casson and Carreau-Yasuda non-Newtonian blood models in steady and oscillatory flows using the lattice Boltzmann method. *Physics of Fluids* 19, 1-13.

Casas, B., J. Lantz, P. Dyverfeldt and T. Ebbers (2016). 4D flow MRI-based pressure loss estimation in stenotic flows: evaluation using numerical simulations. *Magnetic Resonance in Medicine* 75, 1808-1821.

Cherdron, W., F. Durst and J. H. Whitelaw (1978). Asymmetric flows and instabilities in symmetric ducts with sudden expansions. *Journal of Fluid Mechanics* 84, 13-31.

Das, T. and S. Chakrabarti (2015). Flow Characteristic Study in a Configuration of Sudden Expansion with Central Restriction and Fence-Viewed as an Annular Flow Dump Combustor, *Journal of Applied Fluid Mechanics* 8(4), 713-725.

Durst, F., A. Melling and J. H. Whitelaw (1974). Low Reynolds number flow over a plane symmetrical sudden expansion. *Journal of Fluid Mechanics* 64, 111-128.

Edussuriya, S. S., A. J. Williams and C. Bailey (2004). A cell-centred finite volume method for modelling viscoelastic flow. *Journal of Non-Newtonian Fluid Mechanics* 117, 47-61.

Fattah, A. (2012). Control of the Separation Flow in a Sudden Enlargement. *Journal of Applied Fluid Mechanics* 5(1), 57-66.

Fearn, M. R., T. Mullin and A. K. Cliffe (1990). Nonlinear flow phenomena in a symmetric sudden expansion. *Journal of Fluid Mechanics* 211, 595-608.

Ferziger, J. H. and M. Peric (2001). *Computational Methods for Fluid Dynamics*, Springer-Verlag.

Haase, S. A., A. J. Wood, J. M. L. Sprakel and R. G. H. Lammertink (2017). Inelastic non-Newtonian flow over heterogeneously slippery surfaces. *Physical Review* 95(2), 1-11.

Hammad, J. K., G. C. Vradis and V. M. tgen (2001). Laminar Flow of a Herschel-Bulkley Fluid Over an Axisymmetric Sudden Expansion. *Transactions of the ASME* 123, 588- 594.

Joseph, A. S. and F. E. Allen (1996). *Handbook of Fluid Dynamics and Fluid Machinery*, Wiley, 2005-2018.

Konoplev, A. A., G. G. Aleksanyan and L. B. Rytov (2007). Convective heat transfer in channels with high wall ribs. *Theoretical Foundations of Chemical Engineering* 41, 526-532.

Leonard, P. B (1979). A stable and accurate convective modeling procedure based on quadratic upstream interpolation. *Computer Methods in Applied Mechanics and Engineering* 19, 59-98.

Liepsch, D. (2002). An introduction to biofluid mechanics-basic models and applications. *Journal of Biomechanics* 35, 415- 435.

Litvinenko, A. Y., G. R. Grek, G. V. Kozlov, C. A. Serra and G. Martin (2014). Dispersive mixing efficiency of an elongational flow mixer on PP/EPDM blends: Morphological analysis and correlation with viscoelastic properties. *Polymer Engineering & Science* 54, 14-34.

Mao, X., S. J. Sherwin and H. M. Blackburn (2011). Transient growth and bypass transition in stenotic flow with a physiological waveform. *Theoretical and Computational Fluid Dynamics* 25, 31-42.

Mandal, K. D., K. N. Manna and S. Chakrabarti (2011). Influence of primary stenosis on secondary one and vice versa in case of double stenosis. *Journal of Applied Fluid Mechanics* 4 (4), 31-42.

Marn, J. and P. Ternik (2003). Use of quadratic model for modelling of fly ashwater mixture. *Applied Rheology* 13, 286-296.

Menouer, A., N. S. Chemloul, K. Chaib. and A. Kadari (2019). Steady Flow of Purely Viscous Shear-Thinning Fluids in a 1:3 Planar Gradual Expansion. *Journal of Applied Fluid Mechanics* 12(3), 789-801.

Mishra, S. and K. Jayaraman (2002). Asymmetric flows in planar symmetric channels with large expansion ratio. *International Journal for Numerical Methods in Fluids* 38(10), 945-962.

Moallemi, N. and J. Brinkerhoff (2016). Numerical analysis of laminar and transitional flow in a planar sudden expansion. *Computers and Fluids* 140, 209-221.

Motaharinezhad, M., Shahraki, S., Tirgar, R. and H. Bisadi (2014). Numerical investigation of turbulent heat transfer in a sudden expansion fluid flow. *Indian Journal of Scientific Research* 1(2), 47-53.

Moghiman, M., B. Rahmanian, M. R. Safaei and M. Goodarzi (2008). Numerical investigation of heat transfer in circular perforated plates exposed to parallel flow and suction. *International Journal of Advanced Manufacturing Technology* 1(3), 43-56.

Mostafavi, M. and H. A. Meghdadi (2017). New Formulation for Prediction of Permeability of Nano Porous Structures using Lattice Botzmann Method. *Journal of Applied Fluid Mechanics* 10(2),639-649.

Mukhambetiyar, A., M. Jaeger and D. Adair (2017). CFD Modelling of Flow Characteristics in

Micro Shock Tubes. *Journal of Applied Fluid Mechanics* 10(4), 1061-1070.

Nourollahi, I., B. Zafarmand, M. R. Safaei and Y. Maghmoumi (2008). An investigation of lid driven cavity flow by using large eddy simulation. *International Journal of Advanced Manufacturing Technology* 2(1), 25-36.

Patankar, S. V. (1980). *Numerical Heat Transfer and Fluid Flow*, Taylor & Francis.

Peterson, S. D. and M. W. Plesniak (2008). The influence of inlet velocity profile and secondary flow on pulsatile flow in a model artery with stenosis. *Journal of Fluid Mechanics* 616, 263-301.

Petersson, S., P. Dyverfeldt, J. Sigfridsson, J. C. Lantz and T. Carlhll Ebbers (2016). Quantification of turbulence and velocity in stenotic flow using spiral three-dimensional phase-contrast MRI. *Magnetic Resonance in Medicine* 75, 1249-1255.

Neofytou, P. and D. Drikakis (2003). Non Newtonian flow instability in a channel with a sudden expansion. *Journal of Non-Newtonian Fluid Mechanics* 111, 127-150.

Oliveira, J. P. (2003). Asymmetric flows of viscoelastic fluids in symmetric planar expansion geometries. *Journal of Non-Newtonian Fluid Mechanics* 114, 33-63.

Oliveira, N. S. M., L. E. Rodd. and G. H. McKinley (2008). Simulations of extensional flow in microrheometric devices. *Microfluidics and Nanofluidics* 5(6), 809-826.

Pitton, G., A. Quaini. and G. Rozza (2017). Computational reduction strategies for the detection of steady bifurcations in incompressible fluid dynamics: Applications to Coanda effect in cardiology. *Journal of Computational Physics* 334, 534-557.

Poole, J. R., M. A. Alves, P. J. Oliveira and F. T. Pinho (2007). Plane sudden expansion flows of viscoelastic liquids. *Journal of NonNewtonian Fluid Mechanics* 146, 79-91.

Quadros, J. D., S. A. Khan and A. J. Antony (2018). Study of Effect of flow parameters on base pressure in a suddenly expanded duct at supersonic Mach number regimes using CFD and design of experiments. *Journal of Applied Fluid Mechanics* 11, 483-496.

Quadros, D. J. and S. A. Khan (2020). Prediction of Base Pressure in a Suddenly Expanded Flow Process at Supersonic Mach Number Regimes using ANN and CFD. *Journal of Applied Fluid Mechanics* 13(2), 499-511.

Rezaei, M., A. R. Azimian and D. Toghraie (2015). Molecular dynamics study of an electro-kinetic fluid transport in a charged nanochannel based on the role of the stern layer. *Physica A: Statistical Mechanics and its Applications* 426, 25-34.

Ringleb, A., W. Schlter, O. Sommer and G. Wozniak (2018). Large Scale Fluctuations in an Axisymmetric Sudden Pipe Expansion with Large Aspect Ratio. *Journal of Applied Fluid Mechanics* 11(4), 877-883.

Nourollahi, I., B. Zafarmand, M. R. Safaei and Y. Maghmoumi (2008). An investigation of lid driven cavity flow by using large eddy simulation. *International Journal of Advanced Manufacturing Technology* 2(1), 25-36.

Saha, S., P. Biswas and S. Nath (2020). Bifurcation phenomena for incompressible laminar flow in expansion channel to study Coanda effect, *Journal of Interdisciplinary Mathematics* 23(2), 493-502.

Safaei, M. R, B. Rahmanian and M. Goodarzi (2011). Numerical study of laminar mixed convection heat transfer of power-law non-Newtonian fluids in square enclosures by finite volume method. *International Journal of Physical Sciences* 6(33), 7456-7470.

Ternik, P. (2010). New contributions on laminar flow of inelastic non-Newtonian fluid in the two-dimensional symmetric expansion: Creeping and slowly moving flow conditions. *Journal of Non-Newtonian Fluid Mechanics* 165, 1400-1411.

Ternik, P. (2009). Planar sudden symmetric expansion flows and bifurcation phenomena of purely viscous shear-thinning fluids. *Journal of Non-Newtonian Fluid Mechanics* 157, 15-25.

Ternik. P., J. Marn and Z. Zunic (2006). Non-Newtonian Fluid Flow through a Planar Symmetric Expansion: Shear-thickening Fluids. *Journal of Non-Newtonian Fluid Mechanics* 13, 136-148.

Torres, M. J., J. Garca and Y. Doce (2020). Numerical Study of Particle Dispersion in the Turbulent Recirculation Zone of a Sudden Expansion Pipe using Stokes Numbers and Mean Drift Parameter. *Journal of Applied Fluid Mechanics* 13(1), 15-23.

Tsai, H. C., H. T. Chen, Y. A. Wang, H. C. Lin and M. L. Fu (2007). Capabilities and limitations of 2-dimensional and 3-dimensional numerical methods in modeling the fluid flow in sudden expansion microchannels. *Microfluid Nanofluid* 3, 13-18.

Vtel, J., A. Garon, D. Pelletier and M. I. Farinas (2008). Asymmetry and transition to turbulence in a smooth axisymmetric constriction. *Journal of Fluid Mechanics* 607, 351- 386.

Vinogradov, I., L. Khezzar and D. Siginer (2011). Heat transfer of non-Newtonian dilatant power law fluids in square and rectangular cavities. *Journal of Applied Fluid Mechanics* 4 (3), 37-42.